JCIM JOURNAL OF CHEMICAL INFORMATION AND MODELING

pubs.acs.org/jcim
Application Note

MOFSynth-ADV: An Open-Source Engine for Synthesizability Evaluation of Metal−Organic Frameworks

Charalampos G. Livas, Emmanuel Klontzas, Pantelis N. Trikalitis, and George E. Froudakis*

Cite This: https://doi.org/10.1021/acs.jcim.6c00880
Read Online

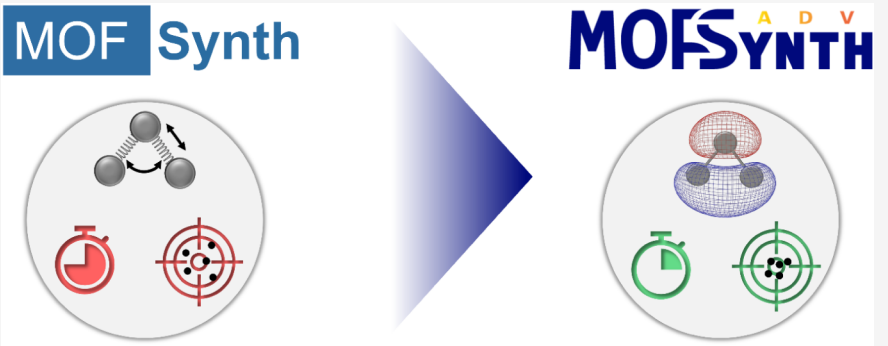

ABSTRACT: We present MOFSynth-ADV, an advanced iteration of the MOFSynth tool designed to evaluate the synthetic feasibility of Metal−Organic Frameworks (MOFs). By integrating the Atomic Simulation Environment (ASE) to leverage extended tight-binding (xTB) and machine learning interatomic potential (MLIP) calculations, MOFSynth-ADV achieves geometry optimization and energy evaluations with significantly higher accuracy than classical force field approaches. Crucially, this update eliminates reliance on proprietary software, delivering a fully open-source solution optimized for high-throughput screening. Performance benchmarks reveal that the xTB module reduces unconverged cases by 73% while decreasing computational time by 13%, with MLIPs (specifically MACE-OFF) yielding comparable improvements. Validated against a benchmark set of experimentally reported MOFs, MOFSynth-ADV demonstrates superior structural and energetic prediction quality, effectively capturing the subtle chemical interactions essential for accurate synthesis prediction. Fast, modular, and easily deployable, this upgraded framework establishes a robust foundation for future machine learning and quantum-classical hybrid workflows in MOF discovery.

INTRODUCTION

The accelerating pace of discovery in the field of metal−organic frameworks (MOFs)[1] is largely enabled by computational pipelines that allow the high-throughput screening of millions of hypothetical materials.[2,3] Among these, MOFSynth[4] emerged as a valuable tool that enables early stage assessment of synthetic feasibility by quantifying the geometric and energetic distortions of linkers upon MOF assembly. This approach addresses a critical gap in the virtual screening workflow, which is the identification of MOF candidates not only with desirable properties, but also with realistic synthetic accessibility.

The original MOFSynth implementation was built around classical force field-based optimization protocols, using the Universal Force Field (UFF)[5] model and Turbomole,[6] which provided the speed and scalability needed for large-scale deployment across databases such as QMOF,[7,8] CoRE MOF,[9] and ToBaCCo.[10] However, the reliance on classical approximations introduced well-known limitations, including inadequate treatment of electron delocalization, hydrogen bonding, and subtle torsional effects,[11] all of which may influence the real-world viability of a given linker within a coordination framework.

In response to the limitations of previous methods, we present MOFSynth-ADV, a substantial evolution of the original platform. This new architecture integrates the Atomic Simulation Environment (ASE)[12] with different calculation methods, such as GFN2-xTB, and machine learning interatomic potentials (MLIPs) like MACE-OFF[13] and MACE-MP.[14] This significantly enhances the accuracy of energy and geometry predictions without sacrificing computational efficiency. There is also a variety of optimizers for the user to choose from (e.g., LBFGS, BFGS, Sella,[15] FIRE[16]).

Received: March 21, 2026
Revised: April 22, 2026
Accepted: April 24, 2026

Table 1. Comparative Performance Statistics of the Classical and Quantum-Mechanical Versions of MOFSynth

Method	Run Time (s)	Δ Time	Total Cases	Non-Converged Cases	Δ Non-Conv
MOFSynth (CL)	19.892	−13%	3.450	367	−73%
MOFSynth-ADV (QM)	17.349		3.450	99	

Together, these methods offer a robust trade-off between fidelity and speed; they capture key quantum mechanical effects while remaining faster. These features make ASE an ideal engine for high-throughput screening pipelines aimed at capturing the subtle energetics that govern synthetic viability.

MOFSynth-ADV replaces the force field engine of the original MOFSynth implementation with an ASE-based optimization framework. The resulting pipeline preserves the tool's core philosophy by evaluating linker deformation and energetic strain between the free and bound conformations but now does so with greater accuracy and improved robustness across diverse chemical moieties. This architecture introduces the following three principal advancements.

First, the newly introduced methods deliver enhanced accuracy by explicitly accounting for electronic effects, such as hydrogen bonding and π-conjugation, which remain inaccessible to classical force fields.[11] Importantly, this quantum mechanical rigor is achieved while retaining computational efficiency comparable to classical methods.

Second, MOFSynth-ADV ensures complete open-source autonomy. By leveraging the Atomic Simulation Environment which is freely available, cross-platform, and straightforward to install. The framework eliminates any reliance on commercial licenses or proprietary force fields. Combined with minimal user input requirements, this simplified deployment guarantees that the tool is broadly accessible to computational and experimental scientists alike.

Finally, the design facilitates a smooth experience for existing users through a restructured web application. The updated MOFSynth interface is highly adaptable, allowing users to easily select the optimal level of theory based on the specific needs of their study.

This Application Note details the updated methodology, the integration strategy, and its implications for synthetic likelihood predictions. We chose to benchmark MOFSynth-ADV utilizing GFN2-xTB with the LBFGS optimizer, against the original version across randomly selected MOF structures from the three databases QMOF, CoRE MOF and ToBaCCo, highlighting differences in energy estimations, structural deviations, and synthesizability classifications. Finally, we showcase the improved performance in handling complex linkers, positioning MOFSynth-ADV as a next-generation solution for synthesis-aware computational screening in reticular chemistry.

METHODOLOGY

The workflow begins with the automated extraction of the MOF's ligand, which is subsequently optimized to identify its most stable conformation. The resulting energy difference ($\Delta E = E_{strained} - E_{relaxed}$) and structural divergence (RMSD) between the framework-bound (strained) conformation and free-gas optimized monomer serve as a reliable estimate of the framework's synthesizability.

In the original implementation, users begin by preparing a working directory containing a folder of CIF input files and a configuration folder with a YAML control file and a shell script for cluster submission. An example directory layout is shown in Figure S1. This extension, MOFSynth-ADV, totally abolishes this need. Only the CIF file(s) is required. The recommended directory structure is shown in Figure S2. Execution follows the same pattern as the classical version, and the output is a consolidated XLSX file.

To showcase the advantages of the new version, we conducted a comparative study between the two versions of MOFSynth. For MOFSynth-ADV, input structures were prepared in XYZ format. Optimizations were executed using GFN2-xTB and the LBFGS optimizer, producing energetically minimized structures suitable for downstream analysis. For comparison, classical Universal Force Field optimizations using the Turbomole suite were also performed.

All calculations were logged to output files to verify convergence. During the fragmentation procedures, a supercell threshold of 20 Å was applied; meaning that if a material's unit cell dimensions fell below this limit, a supercell was constructed to exceed it. Additionally, a fragmentation time limit of 25 s was imposed to accelerate the overall calculations. Initial benchmarks used standard software defaults for geometry optimization: a gradient convergence of 10^{-4} a.u. for UFF-Turbomole and 10^{-3} a.u. for GFN2-xTB. In the current MOFSynth-ADV release, all methods are standardized via the ASE framework with an identical fmax of 0.05 eV/Å to ensure direct comparability.

All calculations were performed on a high-performance computing cluster equipped with 4 × Intel Xeon Gold 6448H processors (32 cores per socket, up to 4.1 GHz), totaling 128 CPU cores per node, running under Debian GNU/Linux 13 and managed via the SLURM workload manager.

RESULTS AND DISCUSSION

To assess the computational performance and robustness of the new tool, we conducted a head-to-head comparison between the original classical force-field (CL) implementation and the advanced (QM) approach, utilizing GFN2-xTB with the LBFGS optimizer. We used an identical data set of 3,450 randomly selected MOF structures drawn from the QMOF, CoRE MOF, and ToBaCCo repositories. Both workflows were executed on the same hardware configuration to ensure a direct and unbiased evaluation of speed and convergence behavior.

As seen in Table 1, the semiempirical QM protocol powered by GFN2-xTB completed the full workflow in 4 h 49 m 9 s (17.349 s), which is approximately 5.02 s per material, compared with 5 h 31 m and 32 s (19.892 s) and 5.76 s per material for the CL engine. This corresponds to a 13% reduction in total wall-time, underscoring the greater suitability of MOFSynth-ADV for large-scale, high-throughput deployment. Similar improvement was seen when using MACE-OFF as seen in Table S3.

Beyond raw speed, MOFSynth-ADV demonstrated a pronounced advantage in numerical stability. The quantum mechanical engine produced only 99 nonconverged energy optimizations, compared with 367 in the classical workflow, as shown in Table 1. This represents a 73% reduction in failed energy calculations, translating to ≈10% more fully converged

https://doi.org/10.1021/acs.jcim.6c00880
J. Chem. Inf. Model. XXXX, XXX, XXX−XXX

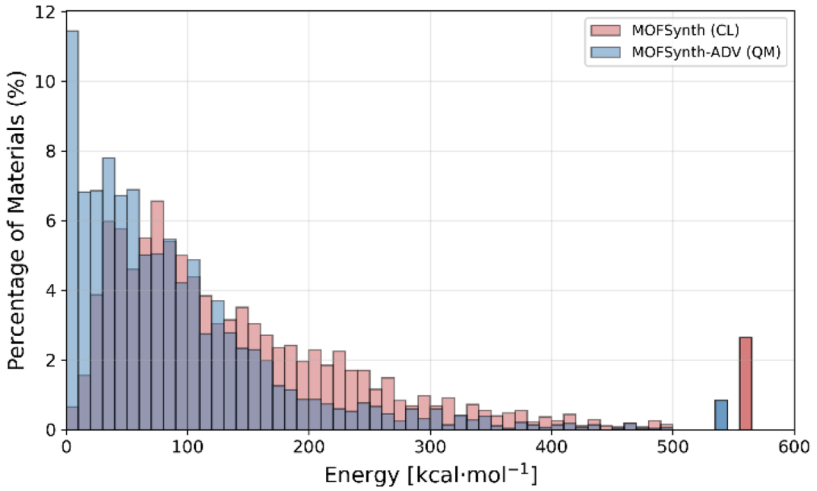

Figure 1. Percentage of materials vs their corresponding energy difference (ΔE) in kcal·mol^{-1} from the two different methods employed.

cases for the same data set. Such a gain is critical for database-scale screening, where even modest improvements in convergence dramatically reduce the need for manual postprocessing or reruns. Further analysis for the three different databases can be found in the Supporting Information.

These findings highlight a key strength of the xTB integration: greater quantum mechanical fidelity delivered with both higher speed and superior structural robustness. In practice, this allows users to process larger databases or allocate saved computational resources to more sophisticated downstream analyses without sacrificing accuracy or reproducibility.

The distributions of the conformational energy difference (ΔE), calculated for the linker in its MOF-bound state versus its optimized gas-phase geometry, are compared for the two MOFSynth versions in Figure 1. The comparison illustrates a clear shift toward lower energy differences in the QM results, indicating a more consistent and physically realistic energetic description across the evaluated structures. In particular, the advanced version predicts a higher proportion of materials with ΔE values clustered in the low-energy region, while significantly reducing the occurrence of large deviations above 500 kcal·mol^{-1}. In contrast, the classical implementation exhibits approximately three times more cases in this high-energy regime, reflecting its tendency to overestimate strain energies in certain frameworks.

To complement the energy diagram, the comparative energy statistics are presented in Table S1. These reveal that both the median and average ΔE obtained from the advanced version are notably smaller than those of the classical counterpart. Furthermore, the maximum energy deviation in the QM data set is considerably reduced, indicating a more stable and physically meaningful energy distribution.

Overall, the distribution of ΔE values and the ΔE statistics demonstrate that the xTB-based approach provides a smoother, more balanced energy landscape, minimizing outlier behavior and yielding results that better reflect the expected energetic stability of experimentally synthesizable MOFs.

In contrast, the root-mean-square deviation (RMSD) statistics summarized in Table S2 show no major structural deviations between the two implementations. As anticipated, both classical and QM optimizations converge toward similar geometries, with only marginal variations in median and average RMSD values. This result reinforces the notion that the key improvement introduced by the new engine lies in the energetic fidelity rather than in altering the structural topology. The near-identical geometric outcomes validate the robustness of the original structural prediction pipeline while highlighting that the updated MOFSynth-ADV provides a more physically consistent energetic landscape without compromising computational efficiency.

The above statistical analysis confirms that the newly introduced workflow produces energetically more realistic values while maintaining geometric fidelity comparable to the classical approach. This critical divergence, where similar optimized structures lead to vastly different energy estimates, is starkly illustrated by the case of QMOF-f85239d (Figure S4). For this framework and others like JIVSIQ_clean (Figure S5), the classical force field calculates an unphysical energy difference (>3000 kcal·mol^{-1}), whereas the QM method yields a chemically reasonable value (36 kcal·mol^{-1}), underscoring a fundamental limitation of the classical potential. A full analysis of these representative cases is provided in the Supporting Information.

To identify the most significant discrepancies between the two approaches, the materials were ranked according to their ΔE obtained from both optimization levels. This process produced two separate rankings, revealing that certain materials were classified as highly synthesizable in one version but poorly ranked in the other. The ten most extreme cases are presented in Table 2. Entries highlighted in green correspond to materials ranked high in the advanced version and low in the CL one, while those in red indicate the opposite trend. This comparison clearly shows the influence of the computational method on the predicted synthesizability ranking.

We manually inspected the linkers corresponding to the five most positive divergent MOFs (green highlight) identified in the ranking analysis. All examined structures contained benzene-based linkers, either unsubstituted or functionalized with nitrogen, oxygen, and terminal oxo-hydrogen groups. In these cases, the CL method consistently failed to reproduce the correct energetic profile, primarily due to geometric distortions. Specifically, the CL optimization displaced the atoms of the functional group out of the molecular plane, while the QM approach maintained a planar and chemically accurate configuration, as illustrated in Figure 2. This observation

https://doi.org/10.1021/acs.jcim.6c00880
J. Chem. Inf. Model. XXXX, XXX, XXX−XXX

Table 2. Top 5 Materials Exhibiting the Largest Differences (Positive and Negative) in Ranking Based on the Calculated ΔE between the Classical and Quantum-Mechanical Versions of MOFSynth

Material	QM Ranking	CL Ranking	ΔRanking
qmof-ae43cc7	373	2756	2383
qmof-1d52386	385	2757	2372
qmof-cc96959	359	2700	2341
qmof-ef677d6	459	2737	2278
qmof-75577f5	532	2694	2162
qmof-cf6922c	2714	644	-2070
qmof-1086d95	2417	381	-2036
qmof-a45ca63	2715	703	-2012
qmof-76ace93	2429	423	-2006
tobmof-9327-_id_158852_	2584	582	-2002

further supports the conclusion that the classical implementation struggles to describe certain linker types accurately.

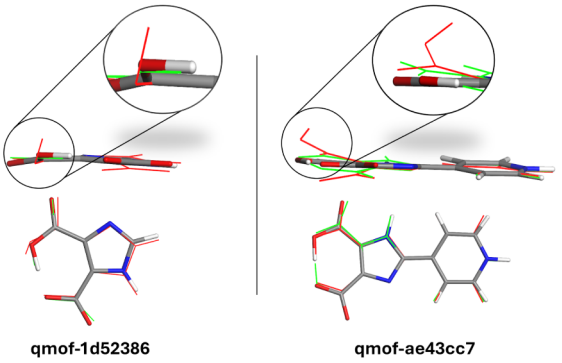

Figure 2. Comparison of two representative MOF cases, qmof-1d52386 (left) and qmof-ae43cc7 (right). The optimized monomer geometries are shown as lines, with green corresponding to the advanced version and red to the CL version, overlaid on the initial unoptimized structure (as sticks) extracted directly from the MOF crystal framework.

Conversely, in cases where the ranking difference between the QM and CL versions was negative, and the QM approach classified a MOF as unsynthesizable, while the CL method predicted it to be synthetically feasible, we observed a consistent pattern related to the nature of the linker. As illustrated in Figure 3, these linkers typically consist of carbon chains with terminal or bridging oxygen atoms. During optimization, the QM calculations often led to bond dissociation, resulting in fragmentation and the formation of carbon dioxide species, whereas the CL approach preserved the molecular connectivity and produced stable geometries with comparable energy values. We repeated the optimization using the hydrogenated monomer to properly terminate the oxygen atoms, however, the results remained unchanged, as illustrated in the lower panel of Figure 3. Furthermore, we anticipate that in some cases these behaviors can emerge when the chemical composition of the linker extracted from the CIF file is

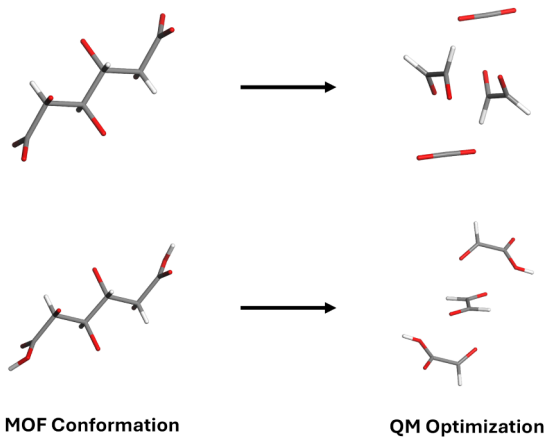

Figure 3. Linker case where the advanced version of the tool fails to calculate the optimized version (top) and the optimization with properly terminated oxygen atoms (bottom).

inaccurate. Other representative examples of this trend include ILIGAL_clean and LASRIJ_clean, which appear to be better described by the classical method in terms of maintaining structural integrity during optimization.

Finally, we examined the cases where the QM workflow yielded particularly large energy differences between the linker monomers. Table 3 presents the ten materials with the highest energy differences in the new version, along with the corresponding values obtained using the CL approach. The results indicate that systems exhibiting unusually high energies in the QM calculations also tend to display elevated energies in the classical ones, suggesting that both methods identify the same problematic cases. Moreover, in several instances, the QM procedure completed the energy evaluation, whereas the classical one failed to converge. Upon closer inspection, it became evident that most of these outliers stem from incorrect or incomplete linker fragmentation, leading to unrealistic molecular fragments. Therefore, it is recommended to apply a greater supercell creation limit, especially in cases of hypothetical MOFs, in order to be sure that a complete representation of the linker is in the unit cell. On top of that, in the analysis part, an upper threshold to the ΔE values, for example, $\Delta E < 500$ kcal·mol^{-1}, is recommended to focus on a range for meaningful interpretation, consistent with the approach used in the original study.

CONCLUSIONS

In this work, we introduced MOFSynth-ADV, an upgraded version of the MOFSynth framework that integrates semi-empirical quantum methods and Machine Learning Potentials to improve the accuracy and reliability of synthetic feasibility predictions for metal−organic frameworks. The transition from a classical force field to a quantum-mechanical engine led to significant performance gains, including a 13% reduction in total computational time and more than 70% decrease in nonconverged calculations across all databases. These improvements establish MOFSynth-ADV as a more stable and efficient platform for large-scale screening of MOF structures.

Benchmark analyses demonstrated that the quantum-mechanical approach provides a more consistent and physically meaningful energy landscape, particularly for linkers containing aromatic or heteroatom-substituted fragments where classical methods often fail to maintain planarity or accurate electronic

https://doi.org/10.1021/acs.jcim.6c00880
J. Chem. Inf. Model. XXXX, XXX, XXX−XXX

Table 3. Ten Materials Exhibiting the Largest Energy Differences Calculated with the Quantum-Mechanical Workflow, along with Their Corresponding Values from the Classical Implementation

Material	QM Energy (kcal·mol^{-1})	CL Energy (kcal·mol^{-1})
INIXOT_clean	−2021	Failed
XONLES01_clean	−894	−1472
ZEDLOL_clean	−887	−795
LOPZAS_clean	−762	−715
YAPSAL_charged	−747	Failed
tobmof-9293-_id_158820_	−719	Failed
tobmof-9991-_id_159518_	−665	Failed
INEBOT01_clean	−654	−1063
BAFCAP_clean	−642	−647
RIFMIE_clean	−626	−1004
tobmof-5646-_id_155172_	−626	−783

distributions. At the same time, both implementations produced comparable optimized geometries, confirming that the key enhancement of the new version lies in the energetic fidelity rather than structural distortion.

The results also highlighted certain cases where the classical method maintained connectivity while the quantum optimization resulted in fragmentation. These cases primarily involve extended carbon−oxygen chains. These instances underline the complementary nature of the two approaches and suggest that careful filtering of high-energy outliers remains essential for reliable interpretation.

Overall, MOFSynth-ADV achieves a balance between quantum-level accuracy, computational efficiency, and full open-source accessibility, removing dependencies on proprietary software and making the tool broadly deployable across platforms. This advancement represents a significant step toward more predictive, synthesis-aware computational screening in reticular chemistry. Future work will focus on coupling the outputs of MOFSynth-ADV with machine learning, further accelerating the discovery of experimentally realizable MOFs.

■ ASSOCIATED CONTENT

Data Availability Statement

We provide our tool in a web interface (https://mofsynth.website), which allows researchers with minimal computational knowledge to use both versions (MOFSynth, MOFSynth-ADV) of our evaluation tool. The source code and example inputs and outputs are available at https://github.com/frudakis-research-group/mofsynth_adv, and the previous version using Classical Force fields is available here https://github.com/frudakis-research-group/mofsynth. All generated files are available in the GitHub repository. The code is distributed under the GNU General Public License v3.0 (GPL-3.0), ensuring that users may run, study, and modify the software while requiring that any derivative works or redistributed versions remain equally open and licensed under the same terms.

Supporting Information

The Supporting Information is available free of charge at https://pubs.acs.org/doi/10.1021/acs.jcim.6c00880.

Software installation and environment setup procedures for classical and advanced versions; directory architectures and configuration file templates for workflow execution; convergence and failure statistics across QMOF, CoRE MOF, and ToBaCCo databases; comparative case studies of structural and energetic discrepancies between force-field and quantum-mechanical methods; comprehensive data tables summarizing energy statistics, RMSD metrics, and computational performance benchmarks (PDF)

■ AUTHOR INFORMATION

Corresponding Author

George E. Froudakis − *Department of Chemistry, University of Crete, Heraklion 71003, Greece;* orcid.org/0000-0002-6907-1822; Email: frudakis@uoc.gr

Authors

Charalampos G. Livas − *Department of Chemistry, University of Crete, Heraklion 71003, Greece;* orcid.org/0000-0002-3340-2239

Emmanuel Klontzas − *Theoretical and Physical Chemistry Institute, National Hellenic Research Foundation, Athens GR-116 35, Greece;* orcid.org/0000-0002-1974-5198

Pantelis N. Trikalitis − *Department of Chemistry, University of Crete, Heraklion 71003, Greece;* orcid.org/0000-0002-6286-2955

Complete contact information is available at: https://pubs.acs.org/10.1021/acs.jcim.6c00880

Author Contributions

C.G.L. was responsible for the conceptualization of the study, performed all calculations, and developed the computational workflow. He conducted the data analysis, generated all figures and tables, and wrote the initial draft of the manuscript. He also contributed to the editing and revision of the manuscript. E.K. provided continuous guidance, technical expertise, and critical insights throughout the project, contributed to the interpretation of results and the refinement of the methodology, and participated in manuscript editing. P.N.T. and G.E.F. contributed to the conceptualization of the study, supervised the research, and provided strategic direction.

Funding

The open access publishing of this article is financially supported by HEAL-Link.

Notes

The authors declare no competing financial interest.

■ ACKNOWLEDGMENTS

The authors would like to acknowledge the financial support from the European Union: Horizon Europe (Project MOST-

H2; Grant Agreement No. 101058547) and Toyota Motor Europe NV/SA. The research work was supported by the Hellenic Foundation for Research and Innovation (HFRI) under the Fourth Call for HFRI PhD Fellowships (Fellowship Number: 9459).

REFERENCES

(1) Yaghi, O. M.; Li, G.; Li, H. Selective binding and removal of guests in a microporous metal−organic framework. *Nature* **1995**, *378*, 703−706.
(2) Fanourgakis, G. S.; Gkagkas, K.; Tylianakis, E.; Froudakis, G. Fast Screening of Large Databases for Top Performing Nanomaterials Using a Self-Consistent, Machine Learning Based Approach. *J. Phys. Chem. C* **2020**, *124*, 19639−19648.
(3) Cao, Z.; Magar, R.; Wang, Y.; Barati Farimani, A. MOFormer: Self-Supervised Transformer Model for Metal−Organic Framework Property Prediction. *J. Am. Chem. Soc.* **2023**, *145*, 2958−2967.
(4) Livas, C. G.; Trikalitis, P. N.; Froudakis, G. E. MOFSynth: A Computational Tool toward Synthetic Likelihood Predictions of MOFs. *J. Chem. Inf. Model.* **2024**, *64*, 8193−8200.
(5) Rappe, A. K.; Casewit, C. J.; Colwell, K. S.; Goddard, W. A.; Skiff, W. M. UFF, a full periodic table force field for molecular mechanics and molecular dynamics simulations. *J. Am. Chem. Soc.* **1992**, *114*, 10024−10035.
(6) TURBOMOLE *Program Package for Electronic Structure Calculations*; TURBOMOLE, https://www.turbomole.org/.
(7) Rosen, A. S.; et al. Machine learning the quantum-chemical properties of metal−organic frameworks for accelerated materials discovery. *Matter* **2021**, *4*, 1578−1597.
(8) Rosen, A. S.; Fung, V.; Huck, P.; O'Donnell, C. T.; Horton, M. K.; Truhlar, D. G.; Persson, K. A.; Notestein, J. M.; Snurr, R. Q. High-throughput predictions of metal−organic framework electronic properties: theoretical challenges, graph neural networks, and data exploration. *Npj Comput. Mater.* **2022**, *8*, 112.
(9) Chung, Y. G.; et al. Advances, Updates, and Analytics for the Computation-Ready, Experimental Metal−Organic Framework Database: CoRE MOF 2019. *J. Chem. Eng. Data* **2019**, *64*, 5985−5998.
(10) Anderson, R.; Gómez-Gualdrón, D. A. Increasing topological diversity during computational "synthesis" of porous crystals: how and why. *CrystEngComm* **2019**, *21*, 1653−1665.
(11) Bannwarth, C.; Ehlert, S.; Grimme, S. GFN2-xTB—An Accurate and Broadly Parametrized Self-Consistent Tight-Binding Quantum Chemical Method with Multipole Electrostatics and Density-Dependent Dispersion Contributions. *J. Chem. Theory Comput.* **2019**, *15*, 1652−1671.
(12) Larsen, A. H.; et al. The atomic simulation environment—a Python library for working with atoms. *J. Phys.: Condens. Matter* **2017**, *29*, 273002.
(13) Kovács, D. P.; et al. MACE-OFF: Short-Range Transferable Machine Learning Force Fields for Organic Molecules. *J. Am. Chem. Soc.* **2025**, *147*, 17598−17611.
(14) Batatia, I.; Benner, P.; Chiang, Y.; Elena, A. M.; Kovács, D. P.; Riebesell, J.; Advincula, X. R.; Asta, M.; Avaylon, M.; Baldwin, W. J.; et al. A foundation model for atomistic materials chemistry. *J. Chem. Phys.* **2025**, *163*, 184110.
(15) Hermes, E. D.; Sargsyan, K.; Najm, H. N.; Zádor, J. Sella, an Open-Source Automation-Friendly Molecular Saddle Point Optimizer. *J. Chem. Theory Comput.* **2022**, *18*, 6974−6988.
(16) Bitzek, E.; Koskinen, P.; Gähler, F.; Moseler, M.; Gumbsch, P. Structural Relaxation Made Simple. *Phys. Rev. Lett.* **2006**, *97*, 170201.

https://doi.org/10.1021/acs.jcim.6c00880
J. Chem. Inf. Model. XXXX, XXX, XXX−XXX